Electronic Supporting Information for:

Detecting and Identifying Reversible Changes in Perovskite Solar Cells by Electrochemical Impedance Spectroscopy

D. Klotz,[1] G. Tumen-Ulzii,[2,3] C. Qin,[2,3] T. Matsushima,[1,2,3] C. Adachi [1,2,3]

[1] International Institute for Carbon Neutral Energy Research (WPI-I2CNER), Kyushu University, Fukuoka, Japan
[2] Center for Organic Photonics and Electronics Research (OPERA), Kyushu University, Fukuoka, Japan
[3] Japan Science and Technology Agency (JST), ERATO, Adachi Molecular Exciton Engineering Project, Fukuoka, Japan
dino.klotz@i2cner.kyushu-u.ac.jp

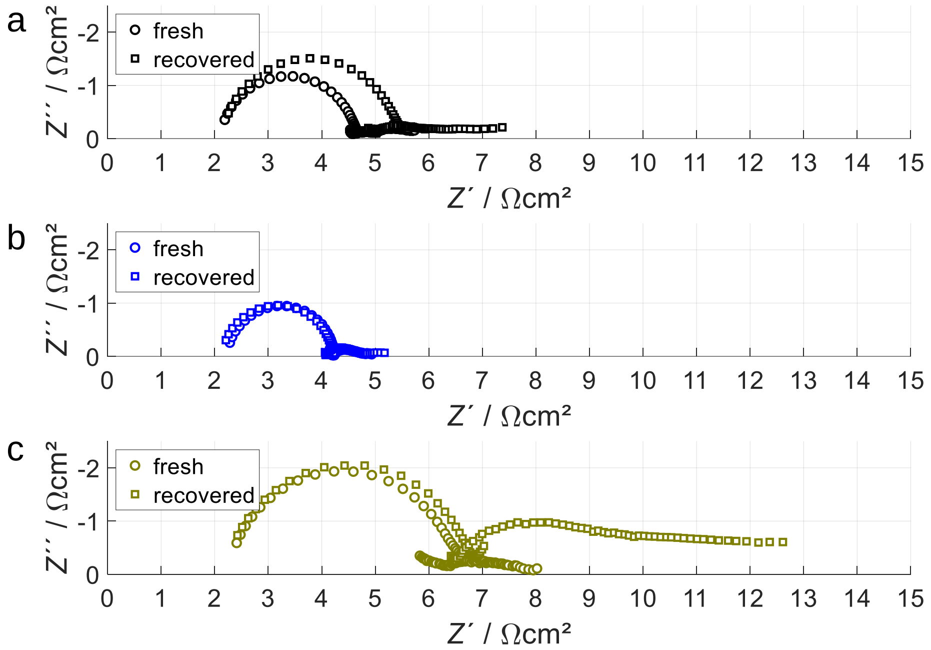

Figure S1. Comparison of fresh and recovered samples as shown in Figure 4 in the main manuscript. This figure shows the full measured frequency range and demonstrates the clear emergence of an intermediate frequency semicircle for the device S-3 with 1.18M PbI_2 in the precurser (lower diagram). This goes along with the degradation seen in the *J-V* curve after the EIS measurement, which is only pronounced for the device S-3 (compare with Figure 4 main manuscript). The gap between high-frequency and low-frequency part originates from the fact that the measurements were conducted separately with a short delay.

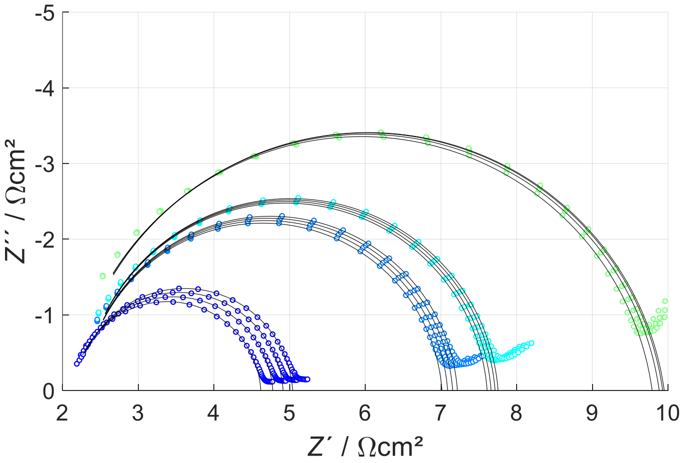

Figure S2. Fitted high-frequency part of the measurements on the fresh sample S-1. Symbols are the measured points; lines represent the fits. The fit parameters can be found in Figure 5 in the main manuscript, the residuals in Figure S7c.

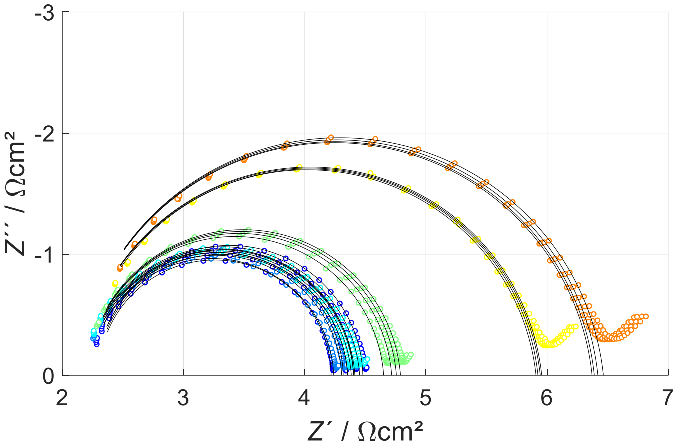

Figure S3. Fitted high-frequency part of the measurements on the fresh sample S-2. Symbols are the measured points; lines represent the fits. The fit parameters can be found in Fig. 5 in the main manuscript, the residuals in Figure S6a.

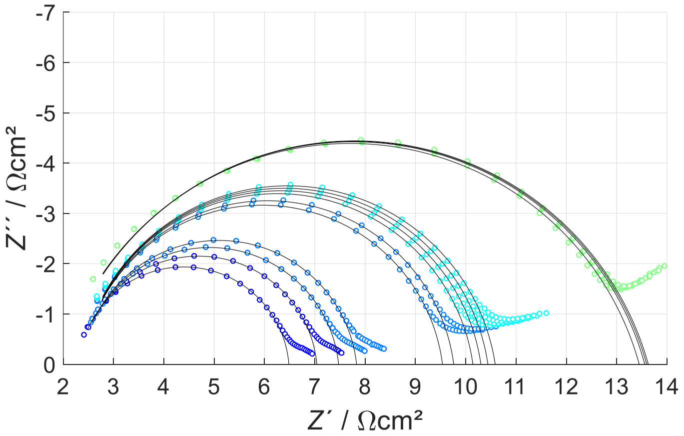

Figure S4. Fitted high-frequency part of the measurements on the fresh sample S-3. Symbols are the measured points; lines represent the fits. The fit parameters can be found in Fig. 5 in the main manuscript, the residuals in Figure S7d.

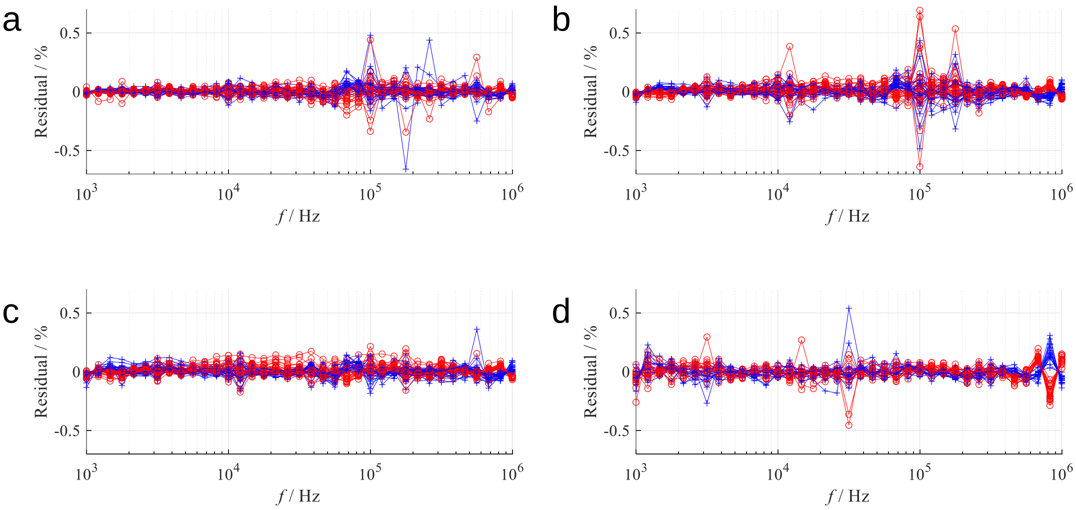

Figure S5. Kramers-Kronig residuals of the measurements on the device S-2. All residuals of the measurements in the respective figure are plotted into one diagram. (a) fresh device (Figure 2, main manuscript); (b) recovered device (Figure 3a, main manuscript); (c) aged device (Figure 3b, main manuscript); (d) aged device measured at ~0.7 V, mimicking stability test conditions (Figure S8, ESI). Apart from single outliers at selected frequencies, the residuals are well below 0.5%, which confirms excellent data quality.

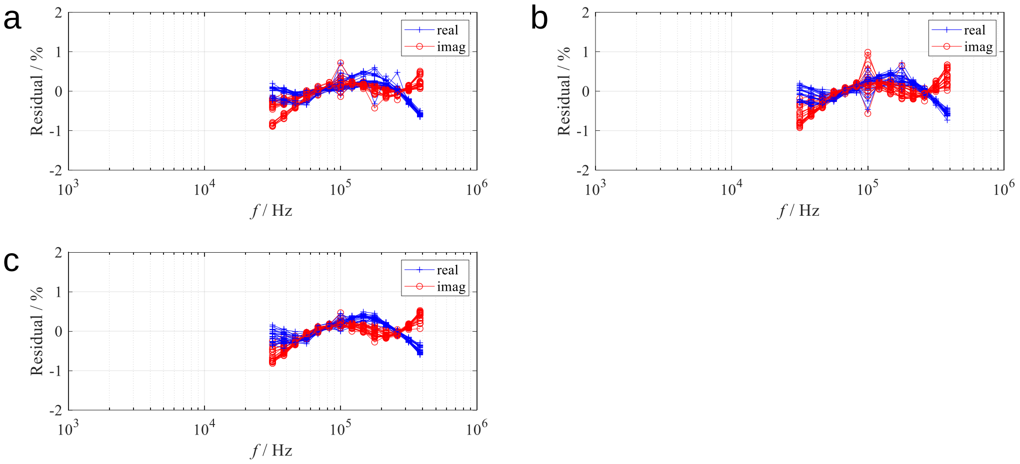

Figure S6. Residuals of the fits on the device S-2. Only the high-frequency data was fitted to the equivalent circuit model (ECM) shown in Figure 4a in the main manuscript. (a) fresh device (Figure 2, main manuscript); (b) recovered device (Figure 3a, main manuscript); (c) aged device (Figure 3b, main manuscript). Single outliers correspond well with the outliers found in Figure S5. Apart from that, there is a systematic deviation towards high frequencies that can be explained by inductivities in the measurement setup, which are reproducible for all fits. Another systematic deviation can be observed towards lower frequencies, which can be explained by the influence of the low frequency semicircle that is not being considered in the ECM but has increasing influence on the impedance towards lower frequencies. In the relevant frequency range, the residuals are well below 1%, which means that the fit results are of very good quality.

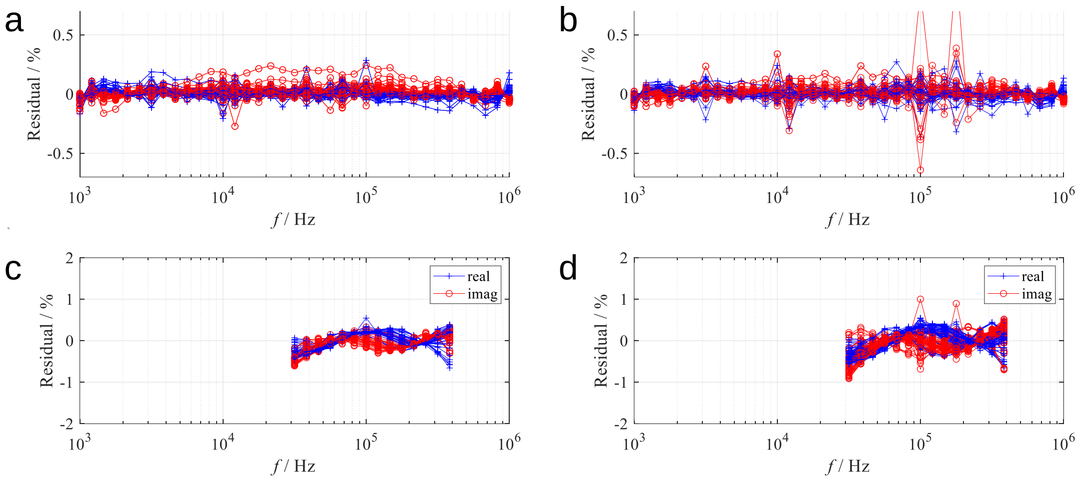

Figure S7. (a, b) Kramers-Kronig residuals and (c, d) residuals of the fits on the device S-1 and S-3. In this figure, all measurements on the devices S-1 and S-5 are plotted in one diagram, respectively. There is a systematic deviation in (a) that represents the time invariance during the first EIS measurement on the recovered sample. EIS measurements on device S-3 exhibit the largest outliers when compared to Figure S6. Apart from that, the overall assessment provided in Figure S6 is valid for the measurements shown here as well.

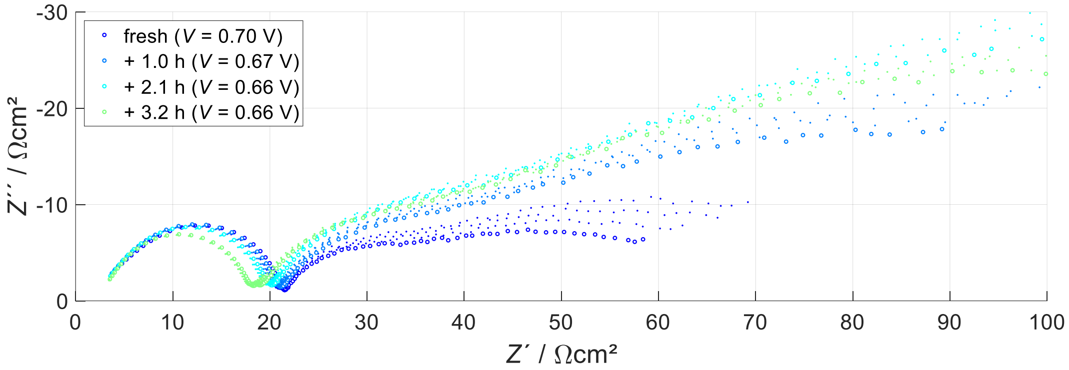

Figure S8. EIS measurements on an additional aged device S-2. The adjusted voltage during the measurement is the voltage that results when the illuminated device is connected to a 1 kΩ resistor. In this operating point, the high-frequency semicircle is showing opposite behaviour as compared to V_{OC} as shown in the main manuscript. The low-frequency behaviour is yet unclear.

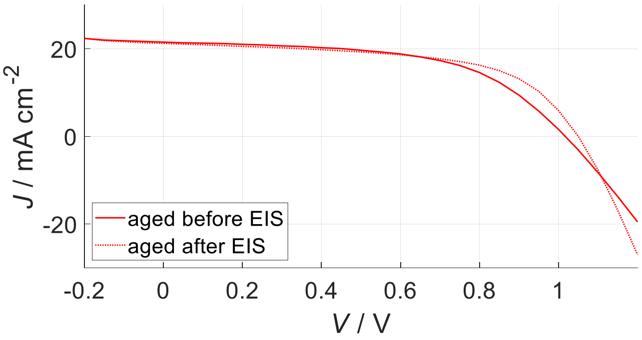

Figure S9. *J*-V curves measured on the additional aged device S-2 before and after the EIS measurements in Figure S8. The apparent inconsistency regarding slope and V_{OC} when comparing Figures S8 and S9 can be explained by the dynamics, as the J-V curve was recorded at 200 mV/s sweep rate, which is much faster than the voltage changes during the EIS measurement below 1 Hz.